Observation of Two-Dimensional Spatial Solitary Waves in a Quadratic Medium

William E. Torruellas, Zuo Wang, David J. Hagan, Eric W. VanStryland, and George I. Stegeman
Center for Research in Electro-Optics and Lasers, University of Central Florida, 12424 Research Parkway, Orlando, Florida 32826

Lluís Torner
Department of Signal Theory and Communications, Polytechnic University of Catalunya, P.O.B. 30002, 08080 Barcelona, Spain

Curtis R. Menyuk
Department of Electrical Engineering, University of Maryland, Baltimore, Maryland 21228-5398
(Received 14 December 1994)

We report the first experimental demonstration of two-dimensional spatial solitary waves in second-order nonlinear optical material. When an intense optical beam is focused into a phase-matchable second-order nonlinear material, the fundamental and generated second-harmonic fields are mutually trapped as a result of the strong nonlinear coupling which counteracts both diffraction and beam walkoff.

PACS numbers: 42.50.Rh

Optical waveguides with an optical response cubic in the optical field have been shown to support one-dimensional temporal or spatial solitons [1,2]. This occurs because dispersion of the optical field can be compensated in space by self-focusing or in time by the effects of self-phase modulation, providing a unique opportunity for the investigation of soliton physics. However, the study of solitons is generally limited in optical experiments to one-dimensional propagation problems. Indeed the governing equation, the cubic nonlinear Shrödinger equation, has been shown mathematically in the two-dimensional case to lead to instabilities and eventual blowup in the paraxial approximation. Experimentally, breakup or catastrophic filamentation of intense optical beams in Kerr media is observed [3]. Even in the nonparaxial case for cylindrically symmetric beams in a medium with a third-order nonlinear ($\chi^{(3)}$) response, propagation results in multiple foci and, therefore, is not solitary (solitonlike) in nature [4]. On the other hand, two-dimensional solitary waves have been proposed in materials with saturable third-order nonlinearities due, for example, to saturable one- and two-photon absorption or electron avalanche ionization [5,6]. To the best of our knowledge they have been demonstrated only in atomic vapors [7]. For completeness we note that other mechanisms such as the photorefractive effect have recently also led to the prediction and demonstration of photorefractive solitons [8].

In all cases the material responds to the presence of the optical field by a nonlinear change in its refractive index. A drastically different approach for the formation of one- and two-dimensional solitary waves involving quadratic nonlinearities ($\chi^{(2)}$) was proposed theoretically as early as 1976 [9]. Recently this approach has been revisited and it has been shown that indeed it is theoretically possible to propagate stable two-dimensional solitary waves in phase-matchable second-order nonlinear materials [10]. In particular, we have predicted that two-dimensional solitary waves form under a variety of experimentally realizable conditions. In this Letter we show experimentally that such effects can indeed be easily implemented under the current state of the art, opening the door to a new opportunity for two-dimensional solitary wave studies.

In second-harmonic generation (SHG), one (type I) or two (type II) input fundamental fields (at frequency ω) mix via $\chi^{(2)}$ to generate a second harmonic (2ω). Because efficient conversion requires wave vector conservation between the interacting beams, dispersion in the refractive index frequently results in different group velocity directions for the interacting beams, leading to "beam walkoff" and reduced SHG. Furthermore, spatial diffraction of the interacting beam also occurs. Here we show experimentally that strong nonlinear coupling can lead to the solitary wave formation of the interacting fields which compensates for diffraction and walkoff and hence allows us to produce clean diffraction-free beams with enhanced peak output intensities. Figure 1 clearly shows that a 20 μm input beam diffracts within the 1 cm length of a KTP crystal when below a certain threshold power when the three fields involved in type II second-harmonic generation in KTP are near phase matching. However, above threshold a clean symmetrical two-dimensional beam is generated for both the fundamental and the second harmonic (not shown here). Thus Fig. 1 proves that solitonlike beams are produced in a second-order process.

Experiments were performed with a 1 cm long KTP crystal cut for type II phase matching along the X-Y plane. In this geometry one of the input fundamental fields is an ordinary field polarized along the Z axis while the second one is an extraordinary field with a polarization in the X-Y plane at the theoretically predicted phase matching angle $\varphi = 26°$. We focused a 1.064 μm beam from a homebuilt, flash lamp pumped, passively mode-locked and Q-switched Nd:YAG laser to a 20 μm waist (half-width at $1/e^2$ in air) at the entrance face of the KTP crystal. In

 0031-9007/95/74(25)/5036(4)$06.00

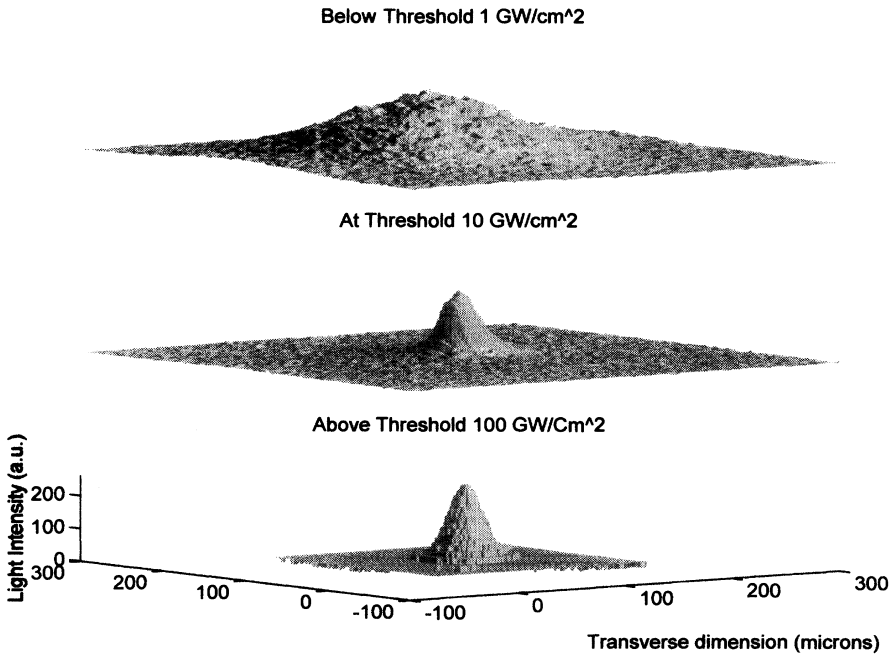

FIG. 1. Two-dimensional plot of the experimentally observed beam profiles at the output of a 1 cm long KTP crystal at optimum phase matching for three input intensities. For intensities above threshold the beam is clamped to a beam waist of 12.5 μm. The three beam profiles were normalized to the same peak value, shown in the bottom figure.

this geometry the linearly polarized input excites two fundamental fields polarized along the Z axis and the extraordinary axis in the X-Y plane. Single 15 psec Gaussian shaped pulses were extracted from the Q-switch envelope with an extracavity electro-optic pulse selector. The focused spot corresponds in KTP to a Rayleigh range (diffraction length) of approximately 2 mm so that the KTP crystal was five diffraction lengths long. A Sensor-Physics laser beam diagnostic camera system, with appropriate linearity correction for the response of the charge coupled device camera, allowed us to view the output beams from the KTP crystal. The input pulse energies were measured with a Laser Precision pyroelectric energy meter placed before the sample, allowing us to measure total energy. Fundamental energy depletions exceeding 50% at phase matching were observed. In order to generate a second-harmonic beam for the seeded experiments, a KDP crystal was used before a 30 cm long gas cell filled with variable pressure nitrogen, allowing us to control the relative phase of the input beams with an accuracy of $\pi/20$. The use of type I KDP keeps the input beams linearly polarized and spatially overlapped.

The governing equations for the three-wave interaction in our type II configuration are

$$\frac{\partial A_1}{\partial z} + \frac{1}{2ik_1}\left(\frac{\partial^2 A_1}{\partial x^2} + \frac{\partial^2 A_1}{\partial y^2}\right) = i\Gamma A_2^* A_3 \exp(-i\Delta k z),$$

$$\frac{\partial A_2}{\partial z} - \rho_\omega \frac{\partial A_2}{\partial x} + \frac{1}{2ik_2}\left(\frac{\partial^2 A_2}{\partial x^2} + \frac{\partial^2 A_2}{\partial y^2}\right) = i\Gamma A_1^* A_3 \exp(-i\Delta k z),$$

$$\frac{\partial A_3}{\partial z} - \rho_{2\omega} \frac{\partial A_3}{\partial x} + \frac{1}{2ik_3}\left(\frac{\partial^2 A_3}{\partial x^2} + \frac{\partial^2 A_3}{\partial y^2}\right) = 2i\Gamma A_1 A_2 \exp(i\Delta k z),$$

where $A_{1,2}$ are the envelopes of the two fundamental fields orthogonally polarized and A_3 is the envelope of the second-harmonic field. $\rho_{\omega,2\omega}$ are respectively the walkoff angles of the extraordinary fundamental and second harmonic with an extraordinary polarization, namely, 0.19° and 0.28° [11]. Γ is the nonlinear coupling coefficient calculated to be 6 cm^{-1} for an input intensity of 1 GW/cm^2 and ΔkL is the phase mismatch [12]. The direction of energy transfer is determined by the sign of the local phase mismatch. In the strong coupling regime the three-wave mixing process is therefore different from the well-known cubic nonlinearity driving the cubic nonlinear Shrödinger equation [12]. The above equations were integrated numerically using a split-step approach, where the linear part was integrated in the Fourier space and the nonlinear part was integrated with a second-order Runge-Kutta algorithm. As shown in Figs. 2(a) and 2(b), numerical predictions are in excellent agreement with our experimental observations, both qualitatively and quantitatively, if the input intensity is scaled up by a factor of 1.5 to correct our CW model for pulsed experiments. The

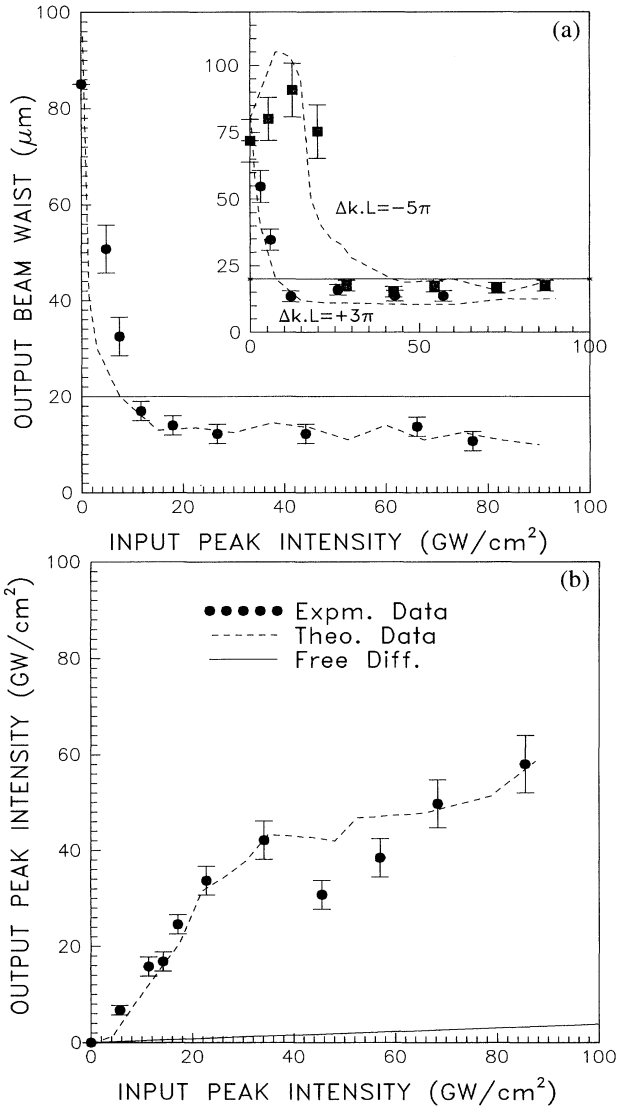

FIG. 2. (a) Measured beam waists are plotted as filled circles. The dashed line shows the prediction of our CW model when the abscissa is scaled by a factor of 1.5. The inset shows the off phase matching cases $\Delta kL = +3\pi$ and $\Delta kL = -5\pi$ as a function of peak intensity in GW/cm^2. The small modulation in our calculation may be due to the 2% numerical error in our propagation code and the fitting of the output profile to a Gaussian one in both laboratory and numeric experiments. The solid line represents the input waist of a freely diffracting beam in air. (b) Measured peak intensity (open circles) at phase matching. The solid line represents the peak intensity of a freely diffracting beam in KTP.

calculations were performed on a PC and the two transverse dimensions and one propagation direction only allowed energy conservation of about 2% in the worst case, adequate for showing good agreement between experiment and theory. These limitations on accuracy could explain some of the small modulation exhibited by the calculations shown in Fig. 2. Our model takes into account depletion of the fundamental and second-harmonic fields, fully reflecting the saturable nature of the nonlinear process. Linear absorption was neglected in such a model at both wavelengths involved. The latter assumption resulted from our transmission measurements at 1064 and 532 nm. Transmission losses were limited by Fresnel reflections at both interfaces.

When the nonlinearity is negligible the expected linear behavior is observed: Both extraordinary waves walk away in space from the ordinary fundamental field and diffraction takes place. Our previous work showed that a positive phase front distortion is present near phase matching and thus induces self-focusing in thick samples, while the saturation mechanism is due to conservation of the total field energy [12]. A close inspection of the governing coupled nonlinear equations shows that, with no second-harmonic input, the second harmonic will try to grow between both fundamentals. Both on the self-focusing side of phase matching and at phase matching the nonlinear interaction progressively changes the output beam profiles as the peak intensities change from 0.1 to 10 GW/cm^2. In this regime self-focusing dominates diffraction, as shown by Fig. 2(a). Down-conversion from the second harmonic to both fundamental fields then occurs. The two fundamental beams start to be trapped by the second harmonic, preventing at higher intensities the mutual walkoff and diffraction. In other words, when back conversion occurs, both fundamental fields try to be located near the peak of the second harmonic. Beyond 5 GW/cm^2 self-focusing along the extraordinary axis takes place eventually trapping the three beams into a cylindrically symmetric solitary wave above 10 GW/cm^2, defeating both diffraction and walkoff. This occurs at a location intermediate to the two original beam centers formed by walkoff of the extraordinarily polarized beam. Figure 2(a) shows that at phase matching the output fundamental beam remains locked to a stable waist of 12.5 μm, almost half of the input waist, clearly showing that diffraction is overcome. Our numerical simulation is also presented. The output profiles, in both the laboratory and numeric experiments, were fitted by Gaussian profiles resulting in the fluctuations observed in Figs. 2(a) and 2(b). Figure 2(b) also shows that the peak intensity is highly enhanced over that of a freely diffracted beam. The above combined effects, good collimation, and high peak intensity are of paramount importance for the use of these beams in subsequent nonlinear optical processes. Note that under appropriate conditions, solitary wave interactions will also occur in a parametric generator or amplifier [13]. A similar evolution into solitary waves is observed on the self-focusing side of phase matching [$\Delta kL > 0$ with the present convention $\Delta k = k_1(\omega) + k_2(\omega) - k_3(2\omega)$], with a lowering of the threshold for solitary wave formation. This is shown in the inset of Fig. 2(a) for a phase mismatch of $+3\pi$ with a 7.5 GW/cm^2 threshold. On the other hand, a very different behavior is observed on the negative side of phase mismatch where self-defocusing occurs first at

powers below a phase mismatch dependent threshold, also shown in the inset of Fig. 2(a). For example, at a phase mismatch of -5π, a threshold intensity of 30 GW/cm^2 is needed for solitonlike beams of 15 to 20 μm diameter to be formed. Based on our modeling this negative phase mismatch behavior may be attributed to waveguiding in the parametric regime. Indeed at these large input powers, during the propagation the second-harmonic field strongly depletes the fundamental fields when it down-converts parametric gain dominates and guides the two fundamental fields which then trap the harmonic field.

A number of simple experiments were performed to further verify that second- and not third-order nonlinearities are responsible for the observed behavior, demonstrating that the latter effects are always negligible under the present experimental conditions. When the fundamental polarization is rotated by 45° the second-harmonic conversion is minimized and no self-focusing effect is observed at even 100 GW/cm^2, indicating that self-focusing due to direct third-order effects was not observable. In other words $\chi^{(3)}$ tensor components are negligible along the principal axis. Similarly with just second-harmonic inputs no beam confinement occurs, as well as for both fundamental and harmonic inputs polarized along one of the principal planes when no significant interaction between the beams occurs, indicating that self-focusing due to diagonal or cross phase modulation tensor components of $\chi^{(3)}$ is also small.

Finally, guided by our numerical simulations which predicted that even on the self-defocusing side of phase matching it is possible to obtain a stable solitary wave under the appropriate seeding with a second harmonic [10], we implemented a seeded experiment with both the fundamental and the second harmonic at approximately the same input intensities. Figure 3 shows that in the regime of self-defocusing ($\Delta kL < 0$), the fundamental beam diffracts to a beam with a waist of 100 μm. However, when the second harmonic with the appropriate phase difference is colaunched, a solitary wave is formed. Again, our numerical simulation is in good agreement with our observation except for the experimentally observed pedestal. When the relative phase is shifted by approximately 180° the solitary beam disappears as predicted. This is additional evidence of a solitary wave being formed in KTP, a quadratic nonlinear optical crystal.

In conclusion, we have unambiguously proven experimentally the formation of two-dimensional solitary waves in a quadratically nonlinear medium. The three waves involved in the experiment mutually trap each other defeating both walkoff and diffraction by producing beams which are in fact compressed in space in comparison with the fundamental input beams. Mutual trapping of the three beams is due to the strong second-order nonlinear coupling, successively up-converting and down-converting the three interacting beams until they become two-dimensional solitary waves. Our results clearly show that solitary waves can be generated over a wide range of physical parameters and are stable when the input intensity is changed over one order of magnitude or the phase matching condition varies over several π around the phase matching resonance.

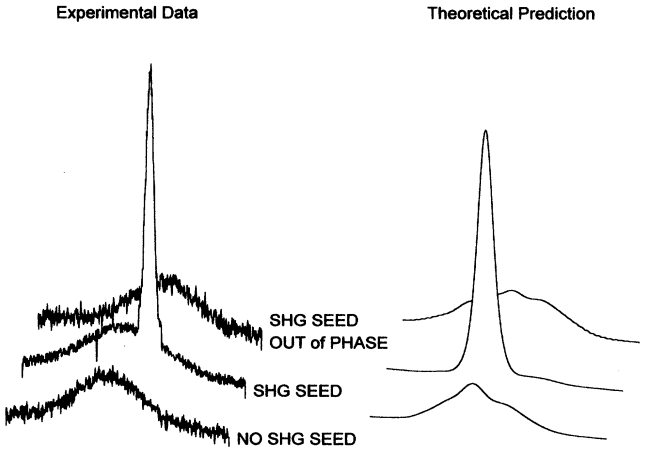

FIG. 3. Beam profile of the fundamental beam in the self-defocusing region, with no second harmonic seeded; with the second harmonic seeded in phase with the fundamental showing the formation of a solitary beam. The relative phase between the two input beams is 180°.

We would like to acknowledge funding for this research provided by ARPA through ARO, and the National Science Foundation.

[1] L. F. Mollenauer, R. H. Stolen, and J. P. Gordon, Phys. Rev. Lett. **45**, 1095 (1980).
[2] A. Barthelemy, S. Maneuf, and C. Froehly, Opt. Commun. **55**, 201 (1985).
[3] See, for example, J. J. Rasmussen and K. Rypdal, Phys. Scr. **33**, 481 (1986); Y. Silberberg, Opt. Lett. **15**, 1282 (1990).
[4] M. D. Feit and J. A. Fleck, J. Opt. Soc. Am. B **5**, 633 (1988).
[5] D. R. Heatley, E. M. Wright, and G. I. Stegeman, Opt. Lett. **56**, 215 (1990).
[6] E. Yablanovitch and N. Bloembergen, Phys. Rev. Lett. **29**, 907 (1972).
[7] J. E. Bjorkholm and A. Ashkin, Phys. Rev. Lett. **32**, 129 (1974).
[8] G. C. Duree *et al.*, Phys. Rev. Lett. **71**, 533 (1993).
[9] Y. N. Karamzin and A. P. Sukhorukov, JETP Lett. **41**, 414 (1976).
[10] L. Torner, C. R. Menyuk, W. E. Torruellas, and G. I. Stegeman, Opt. Lett. **20**, 13 (1995); K. Hayata and M. Koshiba, Phys. Rev. Lett. **71**, 3275 (1993).
[11] B. Boulanger *et al.*, J. Opt. Soc. Am. B **11**, 750 (1994).
[12] See, for example, R. deSalvo, D. J. Hagan, M. Sheik-Bahae, G. I. Stegeman, E. W. VanStryland, and H. Vanherzeele, Opt. Lett. **18**, 28 (1992); G. I. Stegeman, M. Sheik-Bahae, E. W. VanStryland, and G. Assanto, Opt. Lett. **18**, 1397 (1993).
[13] This work is now in progress in our laboratory.

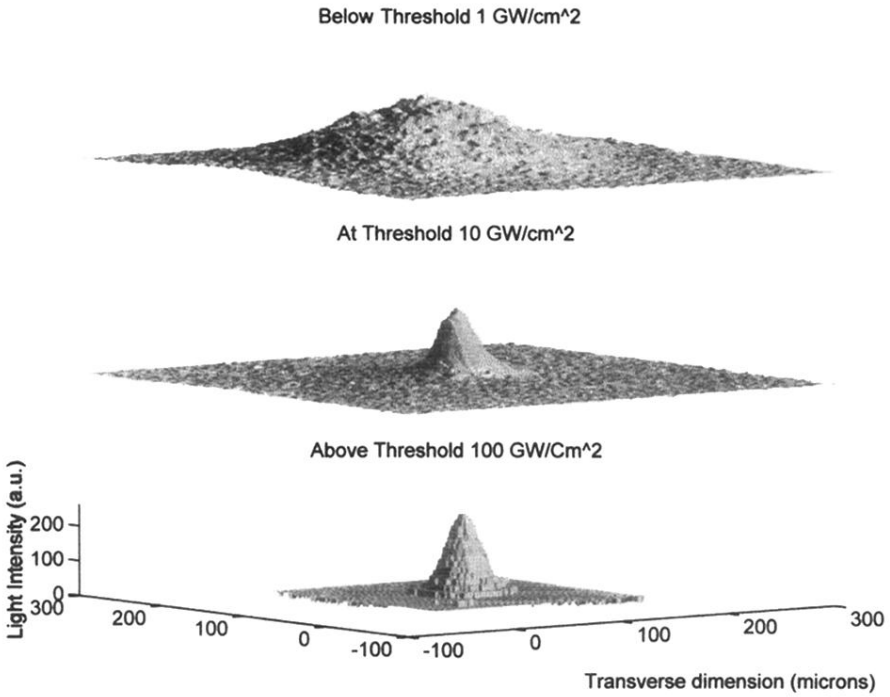

FIG. 1. Two-dimensional plot of the experimentally observed beam profiles at the output of a 1 cm long KTP crystal at optimum phase matching for three input intensities. For intensities above threshold the beam is clamped to a beam waist of 12.5 μm. The three beam profiles were normalized to the same peak value, shown in the bottom figure.